Predictions of laminar flame in aluminium dust clouds with a cylindrical two-dimensional analytical model

M Memarzadeh, M Bidabadi, M Jadidi and A Sedaghat

Proceedings of the Institution of Mechanical Engineers, Part C: Journal of Mechanical Engineering Science 2012 226: 514 originally published online 25 July 2011
DOI: 10.1177/0954406211414999

Predictions of laminar flame in aluminium dust clouds with a cylindrical two-dimensional analytical model

M Memarzadeh[1], **M Bidabadi**[2], **M Jadidi**[2]*, and **A Sedaghat**[1]
[1]Department of Mechanical Engineering, Isfahan University of Technology, Isfahan, Iran
[2]Department of Mechanical Engineering, Iran University of Science and Technology, Tehran, Iran

The manuscript was received on 6 April 2011 and was accepted after revision for publication on 6 June 2011.

DOI: 10.1177/0954406211414999

Abstract: A simple two-dimensional analytical model of laminar flame in aluminium dust clouds is developed for predicting temperature profiles, flame speed, and flammability limit. This study follows previous studies, in which the models were developed in one-dimensional and 2D in Cartesian coordinate forms, and considers cylindrical coordinates since a tubular space is where most of the experimental works on the subject of dust combustion have been carried out. This article aims mainly to study the effect of the heat loss that happens from the surrounding wall on important combustion parameters including the flame speed and lean flammability limit, with more accuracy. The equations are written in the fuel–lean condition and a tube with constant temperature boundary conditions is assumed as well. The zones constructing the structure of a flame include preheat, reaction, and post-flame zones, for which the equations are solved using the method of separation of variables. The model is used to generate a correlation for the variations of flame speeds in terms of particles' diameter, equivalence ratio, and tube diameter. The results show that the flame speed increases with decreasing particle size. It increases with increasing equivalence ratio and the tube diameter, as well.

Keywords: analytical model, aluminium dust cloud combustion, laminar flame speed, lean flammability limit

1 INTRODUCTION

Because of the high heat of combustion, metallic aluminium powders are widely used in high-energy systems: thermite compositions, composite fuels and explosives, and compositions for self-propagating high-temperature synthesis of high-melting compounds [**1**]. While the study of individually burning particles is certainly important, particularly for propellants and explosive applications, another area of practical importance is the study of aluminium dust flames. These types of flames are important in industrial environment, where dust flames are a potentially deadly safety concern, and in propulsion systems where aluminium is combusted with various oxidizers [**2**]. Goroshin *et al.* [**3, 4**] conducted experiments of flame propagation of aluminium dust in a vertical Pyrex tube [**3**] and in a Bunsen-type burner modified for dust cloud combustion [**4**]. These works led to accurate measurements of the flame speed and the quenching distance. The results showed that the flame velocity and quenching distance are weak functions of equivalence ratio in fuel-rich mixtures, and that fuel–lean mixtures are relatively unstable [**3, 4**]. Risha *et al.* [**5, 6**] built an apparatus identical to that of Goroshin and looked at the flame speed in mixtures of micro- and nano-aluminium [**5**] and also in aluminium steam mixtures [**6**]. Shoshin and Dreizin [**7**] also constructed a Bunsen-type dust flame burner using electric fields to aerosolize particles. This study

*Corresponding author: Department of Mechanical Engineering, Iran University of Science and Technology, Tehran, Iran.
email: jadidi_m@yahoo.com

looked at high equivalence ratios (up to 4.5) and showed that flame speed eventually decreased at large equivalence ratios.

Awareness of dynamic parameters (such as the flame thickness, burning velocity, minimum ignition energy, the quenching distance, the flammability limits, and others) gives us extremely valuable information about the basic mechanisms involved in flame propagation in the mixture itself. It is difficult to precisely measure parameters like flame thickness, flammability limits, and the laminar burning velocity and this difficulty is encountered even for premixed gas flames. Thus, researchers have developed theoretical models in an effort to correlate the data in order to gain a better insight into the propagation mechanism involved in the dust flame. A theoretical one-dimensional (1D) model was also proposed by Goroshin *et al.* [**3, 4, 8**]. In this model, it had been supposed that the loss term had linear relation with temperature difference of the gas and the wall. Huang *et al.* [**9, 10**] adapted this model to consider heat loss of the gas to the particles, and Bidabadi *et al.* [**11**] modified this model to consider radiation heat transfer as the mechanism of propagation, while Jadidi *et al.* [**12**] developed this model to obtain quenching distance in a binary suspension of solid fuel particles. This model [**3, 4, 8**] was able to explain the changes in the flame structure based on the individual particles burning time. A two-dimensional (2D) model in a channel was also proposed by Jadidi *et al.* [**13**]. This model [**13**] was a modification of the 1D model [**3, 4, 8**] and temperature variations were considered in both vertical and horizontal axes. The theoretical results for flame speed and lean limit terms obtained by solving equations in the 2D model had much better agreements with experimental results. Considering the fact that the majority of experimental studies on dust combustion have been carried out in a tube, it is necessary to consider the effect of heat loss from the surrounding wall on combustion parameters. Therefore, this study follows the work of Jadidi *et al.* [**13**] and tries to solve partial differential equations in cylindrical coordinate under fuel–lean mixture condition. In the present model, first the diffusion regime is considered for particle combustion and then, an explicit algebraic equation is obtained to predict the flame burning velocity as a function of three variables being the particle size, concentration, and the tube diameter. The variation curve of flame velocity has been used to find lean flammability limits at points where the solution is stable and unstable.

2 MATHEMATICAL MODELING

The starting point for this analysis is the schematic diagram of the flame structure illustrated in Fig. 1. The flame is assumed to propagate in a mixture with considerable excess oxygen (equivalence ratio being smaller than one). There are three distinguished zones in a lean mixture: preheat, flame, and post-flame. In the preheat zone (Zone 1, $-\infty < z < 0$), the reaction rate is small enough to be neglected, the gas being heated by conduction from the flame zone. The surrounding gas heats the particles, elevating their temperature to its ignition point. Goroshin *et al.* [**3**] (also [**8–13**]) assumed the particle temperature at the moment of ignition ($z = 0$), to be close to the auto-ignition temperature of a single particle, T_{si}. It is the diffusive regime in which particles burn in the flame zone, while the particle temperature remains approximately constant [**3, 13**], (Zone 2, $0 < z < v_u\tau_c$). After completion of the combustion, the heat is lost in the post-flame zone until the gas temperature gradually returns to the initial value (Zone 3, $v_u\tau_c < z < +\infty$). Cylinder radius is represented by a, axis z shows the flame's movement direction, and axis r is in the radial direction. All the assumptions existing in the 2D model in Cartesian coordinates [**13**] are made here as well. The chief assumptions and approximations include: (a) a mixture of gaseous oxidizer and aluminium particles which are uniformly distributed and equal-sized is assumed; (b) energies involving the effect of the gravitational force is considered negligible; (c) the flow is laminar, uniform, and steady; (d) the particle velocity is taken to be equal to the gas velocity; and (e) the Biot number of the particles is taken to be negligibly small, meaning the existence of uniform temperature for each particle. It is further assumed that in the diffusive regime of particle combustion, the particle burning rate $\mathrm{d}m_s/\mathrm{d}t$ is directly proportional to the following parameters: local particle radius r_s, the local oxygen concentration C_{o_2}, and the diffusion

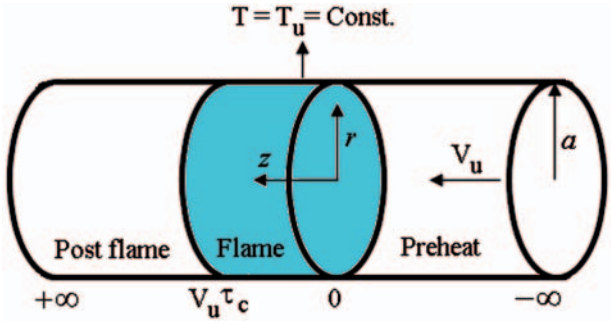

Fig. 1 Schematic sketch of the model adopted

coefficient of oxygen D. The above-mentioned assumptions can be summarized in the following equation [**3**]:

$$\frac{\mathrm{d}m_s}{\mathrm{d}t} \approx D(\bar{T})\, r_s\, C_{o_2} \tag{1}$$

Since the lean mixture has excess oxygen and oxygen diffusivity is weakly dependent on the ambient gas temperature, the total particle burning time in a flame front is approximately equal to the burning time of an individual particle τ_c. Consequently, the term for the heat source is written as in equation (2) for the flame zone using the average burning rate of aluminium particle (m_s/τ_c) [**3, 4, 8–13**]:

$$W_f = \frac{B_u}{\tau_c} Q \tag{2}$$

The equation describing inert particle heating in the preheat zone is (lumped method)

$$v_u m_s C_s \frac{\mathrm{d}T_s}{\mathrm{d}z} = \frac{\lambda_u}{r_s}\left(4\pi r_s^2\right)(T_s - T) \tag{3}$$

where the Nusselt number is taken as a constant equal to 2 and the thermal conductivity of gas, λ, is taken to be constant [**3, 4, 8–13**].

Conservation of energy in the gas flow is given by:

Preheat zone

$$\frac{\partial^2\theta_1}{\partial r^2} + \frac{1}{r}\frac{\partial\theta_1}{\partial r} + \frac{\partial^2\theta_1}{\partial z^2} - 2s\frac{\partial\theta_1}{\partial z} = 0 \tag{4}$$

Flame zone

$$\frac{\partial^2\theta_2}{\partial r^2} + \frac{1}{r}\frac{\partial\theta_2}{\partial r} + \frac{\partial^2\theta_2}{\partial z^2} - 2s\frac{\partial\theta_2}{\partial z} = -N \tag{5}$$

Post-flame zone

$$\frac{\partial^2\theta_3}{\partial r^2} + \frac{1}{r}\frac{\partial\theta_3}{\partial r} + \frac{\partial^2\theta_3}{\partial z^2} - 2s\frac{\partial\theta_3}{\partial z} = 0 \tag{6}$$

The parameters, s, N, θ in the above equations are defined as follows:

$$s = \frac{\rho_u v_u c_p}{2\lambda}, \quad N = \frac{B\,Q}{\lambda\,\tau_c}, \quad \theta = T - T_u \tag{7}$$

with the following boundary conditions:

$$\begin{aligned}
&\theta_1(r, -\infty) = 0, \quad \theta_1(a, z) = 0, \quad \frac{\partial\theta_1}{\partial r}(0, z) = 0,\\
&\theta_1(r, 0^+) = \theta_2(r, 0^-),\\
&\frac{\partial\theta_1}{\partial z}(r, 0^-) = \frac{\partial\theta_2}{\partial z}(r, 0^+), \quad \frac{\partial\theta_2}{\partial r}(0, z) = 0,\\
&\theta_2(a, z) = 0, \quad \theta_2(r, v_u\tau_c^+) = \theta_3(r, v_u\tau_c^-),\\
&\frac{\partial\theta_2}{\partial z}(r, v_u\tau_c^-) = \frac{\partial\theta_3}{\partial z}(r, v_u\tau_c^+), \quad \frac{\partial\theta_3}{\partial r}(0, z) = 0,\\
&\theta_3(a, z) = 0 \quad \theta_3(r, +\infty) = 0
\end{aligned} \tag{8}$$

the above equations are solved using the method of separation of variables [**13–15**] and the following solutions are obtained:

$$\theta_1(r, z) = \sum_{n=1}^{\infty} A_n \exp((s + \sqrt{s^2 + \mu_n^2})z) J_0(\mu_n r) \tag{9}$$

$$\begin{aligned}
\theta_2(r, z) = {} & \frac{1}{2}N\left(a^2 - r^2\right) + \\
& \sum_{n=1}^{\infty} B_n \left(\begin{array}{l} \dfrac{\left(\sqrt{s^2+\mu_n^2} - s\right)}{\left(\sqrt{s^2+\mu_n^2} + s\right)} \dfrac{\exp\left((s - \sqrt{s^2+\mu_n^2})v_u\tau_c\right)}{\exp\left((s + \sqrt{s^2+\mu_n^2})v_u\tau_c\right)} \\ \exp\left((s + \sqrt{s^2 + \mu_n^2})z\right) \\ + \exp\left((s - \sqrt{s^2 + \mu_n^2})z\right) \end{array} \right) J_0(\mu_n r) \\
& + \sum_{n=1}^{\infty} C_n \left(\frac{\left(\sqrt{s^2 + \mu_n^2} - s\right)}{\left(\sqrt{s^2 + \mu_n^2} + s\right)} \exp\left((s + \sqrt{s^2 + \mu_n^2})z\right) \right. \\
& \left. + \exp\left((s - \sqrt{s^2 + \mu_n^2})z\right) \right) J_0(\mu_n r)
\end{aligned} \tag{10}$$

$$\theta_3(r, z) = \sum_{n=1}^{\infty} E_n \exp((s - \sqrt{s^2 + \mu_n^2})z) J_0(\mu_n r) \tag{11}$$

the eigenvalues of which are given by:

$$J_0(\mu_n a) = 0\,, \quad n = 1, 2, 3\ldots \tag{12}$$

Daou and Matalon [**16**] have obtained solutions that are similar in nature (i.e. the exponential terms in the preheat and post-flame regions) using an asymptotic expansion. Maruta *et al.* [**17**] have also found similar exponential solutions for combustion in heated micro-channels. They solved the combustion characteristics for time-dependent, 1D energy equation for flame propagation in a parallel plate configuration.

The first term on the right-hand of equation (10) can be expanded as (Fourier/Bessel series method)

$$\frac{1}{2}N(a^2 - r^2) = \sum_{n=1}^{\infty} F_n J_0(\mu_n r) \tag{13}$$

The constants A_n, B_n, C_n, and E_n are evaluated using the boundary conditions at the flame zone and F_n is obtained using the functions orthogonality theory:

$$\begin{aligned}
A_n &= \frac{\alpha_n}{1 + \alpha_n} F_n(1 - \gamma_n\beta_n)\\
B_n &= \frac{-F_n}{1 + \alpha_n}\left(\gamma_n + \frac{1 - \gamma_n}{1 - \beta_n}\right)\\
C_n &= \frac{F_n}{1 + \alpha_n}\frac{1 - \gamma_n}{1/\beta_n - 1}\\
E_n &= \frac{F_n}{1 + \alpha_n}(\gamma_n - 1)
\end{aligned} \tag{14}$$

where

$$F_n = \frac{N}{\mu_n^2}\frac{J_2(\mu_n a)}{J_1^2(\mu_n a)}$$

$$\alpha_n = \frac{\sqrt{s^2+\mu_n^2}-s}{\sqrt{s^2+\mu_n^2}+s}$$

$$\beta_n = \frac{\exp((s-\sqrt{s^2+\mu_n^2})\nu_u\tau_c)}{\exp((s+\sqrt{s^2+\mu_n^2})\nu_u\tau_c)}$$

$$\gamma_n = \frac{1}{\exp((s-\sqrt{s^2+\mu_n^2})\nu_u\tau_c)} \tag{15}$$

The energy conservation equation for the fuel particle (3) is

$$\frac{\partial\theta_s}{\partial z} = \zeta(\theta_1 - \theta_s) \tag{16}$$

where

$$\zeta = \frac{3\lambda}{r_s^2\rho_s C_s \nu_u} \qquad \theta_s = T_s - T_u \tag{17}$$

with boundary condition

$$z \to -\infty, \quad \theta_s = 0 \tag{18}$$

the equation (16) is solved using the boundary condition (18) and equation (9), and the following solution is obtained:

$$\theta_s(r,z) = \sum_{n=1}^{\infty} \frac{\xi A_n}{\xi + (s+\sqrt{s^2+\mu_n^2})} \exp((s+\sqrt{s^2+\mu_n^2})z)$$
$$J_0(\mu_n r) \tag{19}$$

Furthermore, while the particle temperature in $z = 0$ equals the ignition temperature, T_{si} [**3, 4, 8–13**], subsequently we have:

$$\theta_s(r,0) = \theta_{si} = \sum_{n=1}^{\infty} \frac{\xi A_n}{\xi + (s+\sqrt{s^2+\mu_n^2})} J_0(\mu_n r) \tag{20}$$

where

$$\theta_{si} = T_{si} - T_u \tag{21}$$

θ_{si} is expanded as (Fourier/Bessel series method):

$$\theta_{si} = \sum_{n=1}^{\infty} t_n J_0(\mu_n r) \tag{22}$$

In addition (equations (20) and (22))

$$t_n = \frac{A_n\zeta}{(s+\sqrt{s^2+\mu_n^2})+\zeta} \tag{23}$$

where (making use of the functions orthogonality [**13–15**]) we have:

$$t_n = \frac{2\theta_{si}}{\mu_n a J_1(\mu_n a)} \tag{24}$$

Finally, the exact solution for the temperature profile can be used to obtain a correlation for the variation of flame speed with equivalence ratio. By equating the above two equations (equations (23) and (24)), the key equation of flame speed is obtained:

$$\frac{A_n\zeta}{(s+\sqrt{s^2+\mu_n^2})+\zeta} = \frac{2\theta_{si}}{\mu_n a J_1(\mu_n a)} \quad \Rightarrow$$

$$\varphi = \frac{4\theta_{si}J_1(\mu_n a)\mu_n(\xi+s+\sqrt{s^2+\mu_n^2})\sqrt{s^2+\mu_n^2}}{N\xi a J_2(\mu_n a)(\sqrt{s^2+\mu_n^2}-s)(1-\frac{1}{\exp((s+\sqrt{s^2+\mu_n^2})\nu_u\tau_c)})} \tag{25}$$

3 RESULTS

All the results existing here are very similar to those obtained in the 2D model in Cartesian coordinates [**13, 18**]. The gas (air) temperature profiles in the preheat, the flame, and the post-flame regions are shown in Figs 2 to 4. The diameter of particles and the equivalence ratio are $d_p = 5.4\mu$m and $\phi = 0.7$,

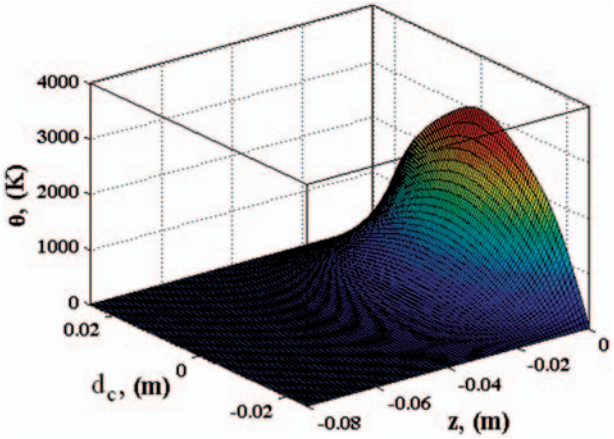

Fig. 2 2D temperature distribution in the preheat region ($-\infty < z < 0$)

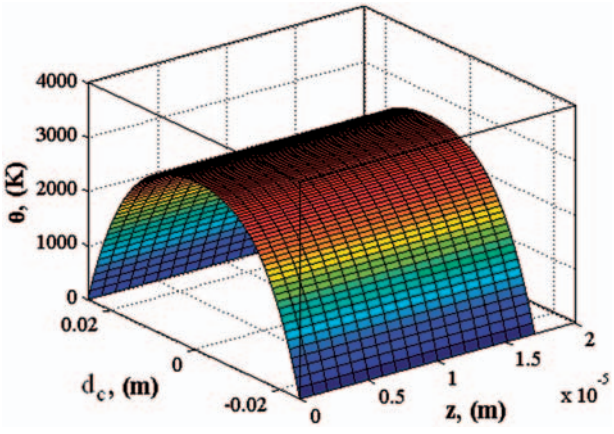

Fig. 3 2D temperature distribution in the flame region ($0 < z < \nu_u\tau_c$)

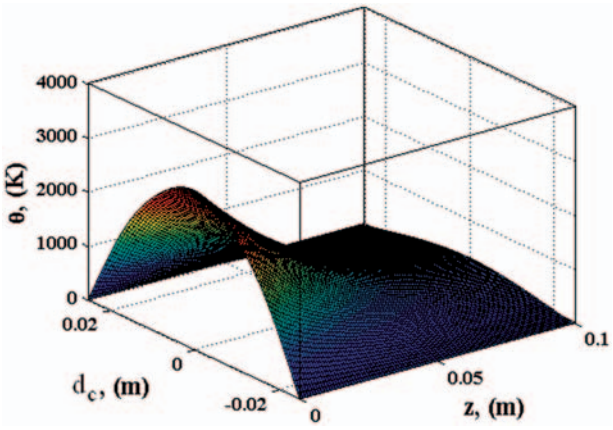

Fig. 4 2D temperature distribution in the post-flame region ($\nu_u \tau_c < z < +\infty$)

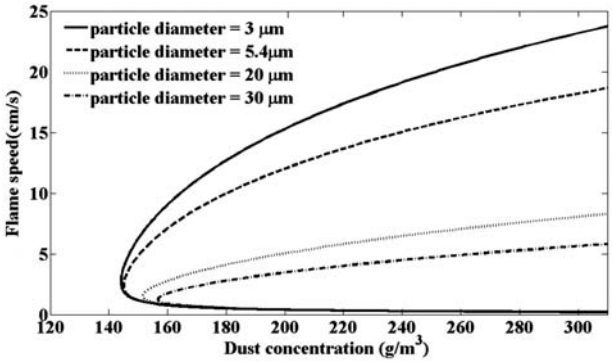

Fig. 5 Effect of particle diameter on flame speed

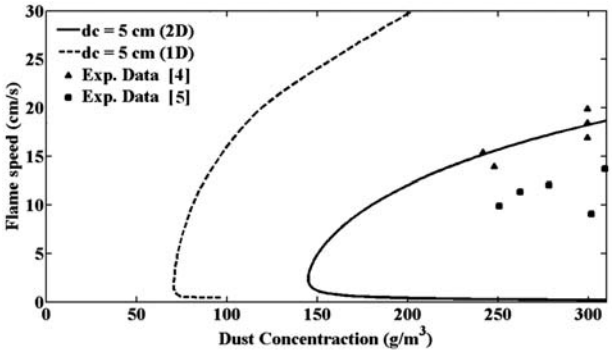

Fig. 6 Comparison between 2D and 1D theoretical flame speeds

respectively. The variations of the temperature along the centre-line of the tube correspond with the temperature curves derived in the 1D models [**9–11**]. Moreover, temperature profiles along the tube width resemble the ones obtained in the 2D model in rectangular coordinates [**13**]. The equation $(-\lambda \frac{\partial T}{\partial r}|_{r=a})$ can be used to obtain heat losses on the tube surface. In the preheat zone, heat is transferred to the gas *via* conduction from the flame zone. In the flame zone, in spite of the fact that this zone is small compared to other zones, gas temperature is approximately constant. In the post-flame zone, the temperature goes down until it finally reaches the initial temperature. Assuming that the particles are uniformly distributed, we obtain that temperature profilesare symmetrical with respect to the tube centre-line. Tube diameter is $d_c = 5$cm and the surface temperature reaches the surrounding temperature at the radius of $r = 2.5$ cm, since it had been assumed ($T = T_u$). In Fig. 5, the laminar flame speeds are shown for various values of particle diameter ($d_c = 5$cm). The dependence of the flame speed on the particle size is quite strong. Experimentally, it is extremely difficult to sustain flame propagation in a suspension of large particle size. For larger particle size, the flame speed is lower than that for smaller particle size. These results are due to the physical structure of the dust flame. The flame speed of a dust–air mixture in the reaction zone is governed by the total surface area available within the reaction zone, which depends on the particle size. Small particles have more surface area per unit volume than larger ones; thus, more fuel available in the reaction zone, consequently a higher value of flame speed. In the present results, in general, two values of flame speed are possible, the lower one is unstable though [**3, 9–13**]. The quenching condition occurs by definition at the critical point of the flame velocity curve (where the two solutions merge, bifurcation point) [**3, 11–13**]. In addition, from the theory, it can be seen that for larger particle size, the lean flammability limit is larger than that of smaller particle size [**3**]. These results are physically meaningful because the burning time of a large particle is greater than that of a smaller one. Also, a large value of burning time corresponds to a thicker flame, and as a result, a larger value of quenching distance. The 1D and 2D flame speed profiles as a function of dust concentration are illustrated in Fig. 6. The validity of 2D results is verified by the experimental results in other previous published works [**4, 5**]. In Fig. 6, the particle diameter is assumed to be 5.4μm. The theoretical value of the lean flammability limit is obtained from the 2D flame speed curve, as 140 g/m^3 (from the 1D flame speed curve, as 68 g/m^3). This value is a little lower than the experimentally obtained value of 157 g/m^3. Figure 7 shows the dependence of the flame speed on the fuel equivalence ratio for different values of the tube diameter ($d_p = 5.4\,\mu$m) for lean mixture. As can be seen, the lean flammability limit grows with reducing tube diameter [**3, 13, 18**] because of the increase of heat transfer rate between the flame and the wall or in fact the increase of heat loss to the wall. With the

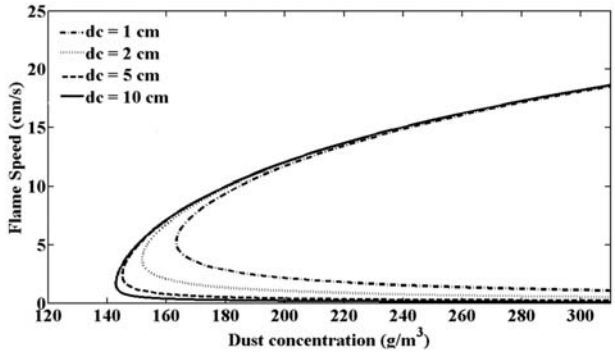

Fig. 7 Effect of tube diameter on flame speed

increase of tube diameter, flame speed increases a little as well [**13**].

4 CONCLUSIONS

Whether it is in the prevention of dust flames and explosions, the use of more efficient and environmentally safe dust combustion, or the improvement of propellants or production of advanced materials, dust combustion research has helped gain an understanding on many of the mentioned issues. Given the important roles that dusts and powders represent in present day industry, fundamental understanding of the basic mechanisms governing heterogeneous combustion is not only necessary but essential to the general field of combustion. Unfortunately, despite its importance, heterogeneous combustion has received only a small fraction of the attention that homogeneous or gas combustion has received in combustion research. Much of this lack of knowledge is attributed to the many complexities involved in heterogeneous or multi-phase combustion and has thus made dust combustion more of an empirical study with very little theoretical understanding of the basic combustion parameters. The laminar flame speed is a very important and fundamental combustion parameter that describes the basic heat and mass transfer processes in a reaction zone. This article has investigated the heat transfer processes in aluminium dust cloud combustion from the theoretical point of view. A simple 2D theory has been developed based on the assumptions of slug flow and constant wall temperature. The exact solutions for temperature profiles and a new algebraic equation for flame speed have been found. This equation can determine the relationship between flame speed and particle diameter, tube diameter, and dust concentration. As shown in the presented figures, the flame speed increases with decreasing particle size and with increasing dust concentration. Compared to the 1D state, the 2D results show more proximity to the experimental results. Particularly lean limit values, flame speed, and flame temperature correspond to the experimental results. The theoretical values of the lean flammability limit and the flame temperature are around 140 g/m^3 and 3300 K respectively ($d_p = 5.4\,\mu$m, $d_c = 5$ cm).

REFERENCES

1 **Gromov, A. A., Popenko, E. M., Sergienko, A. V., Il'in, A. P.,** and **Vereshchagin, V. I.** Nitride formation during combustion of ultrafine aluminum powders in air, I. Effect of additives. *Combust. Explos. Shock Waves*, 2005, **41**(3), 303–314.

2 Bazyn, T. A. *Spectroscopic measurements of the combustion of aluminum and aluminum-based energetic material particles using a heterogeneous shock tube.* PhD Thesis, University of Illinois at Urbana-Champaign, Champaign, IL, 2006.

3 **Goroshin, S., Bidabadi, M.,** and **Lee, J. H. S.** Quenching distance of laminar flame in aluminum dust clouds. *Combust. Flame*, 1996, **105**, 147–160.

4 **Goroshin, S., Fomenko, I.,** and **Lee, J. H. S.** Burning velocity in fuel-rich aluminum dust clouds. *Proc. Combust. Inst.*, 1996, **26**, 1961–1967.

5 **Risha, G. A., Huang, Y., Yetter, R. A.,** and **Yang, V.** Experimental investigation of aluminum particle dust cloud combustion. *Proceedings of the 43rd aerospace sciences meeting and exhibit*, American Institute of Aeronautics and Astronautics, Reno, NV, January 10–13 Paper No. AIAA paper 2005-739.

6 **Risha, G. A., Huang, Y., Yetter, R. A., Yang, V., Son, S.,** and **Tappan, B.** Combustion of aluminum particles with steam and liquid water. In Proceedings of the *44th AIAA aerospace sciences meeting and exhibit*. American Institute of Aeronautics and Astronautics, Reno, NV, January 9–12 Paper No. AIAA paper 2006-1154.

7 **Shoshin, Y.** and **Dreizin, E.** Particle combustion rates in premixed flames of polydisperse metal-air aerosols. *Combust. Flame*, 2003, **133**(3), 275–287.

8 **Goroshin, S., Kolbe, M.,** and **Lee, J. H. S.** Flame speed in a binary suspension of solid fuels particles. *Proc. Combust. Inst.*, 2000, **28**, 2811–2817.

9 **Huang, Y., Risha, G. A., Yang, V.,** and **Yetter, R. A.** Combustion of bimodal nano/micron-sized aluminum particle dust in air. *Proc. Combust. Inst.*, 2007, **31**, 2001–2009.

10 **Huang, Y., Risha, G. A., Yang, V.,** and **Yetter, R. A.** Analysis of nano-aluminum particle dust cloud combustion in different oxidizer environments. In Proceedings of the *43rd aerospace sciences meeting and exhibit*, Reno, NV, January 10–13 AIAA paper 2005-738.

11 **Bidabadi, M., Shabani Shahrbabaki, A.,** and **Jadidi, M.** and **Montazerinejad, S.** An analytical study of radiation effects on the premixed laminar flames of aluminum dust clouds. *Proc. IMechE, Part C:*

J. Mechanical Engineering Science, 2010, **224**, 1679–1695.

12 **Jadidi, M., Bidabadi, M.,** and **Shahrbabaki, A. S.h.** Quenching distance and laminar flame speed in a binary suspension of solid fuel particles. *Lat. Am. Appl. Res.*, 2010, **40**, 39–45.

13 **Jadidi, M., Bidabadi, M.,** and **Hosseini, M. E.** Predictions of laminar flame in aluminum dust clouds with a two-dimensional analytical model. *Proc. IMechE, Part G: J. Aerospace Engineering*, 2009, **223**, 915–925.

14 **Arpaci, V. S.** *Conduction heat transfer*, 1966 (Addison-Wesley, Reading, Massachusetts).

15 **Wylie, C. R.** *Advanced engineering mathematics*, edition 3, 1966 (McGraw-Hill, Kogakusha, New York).

16 **Daou, J.** and **Matalon, M.** Influence of conductive heat losses on the propagation of premixed flames in channels. *Combust. Flame*, 2002, **128**, 321–339.

17 **Maruta, K., Parc, J. K., Oh, K. C., Fujimori, T., Minaev, S. S.,** and **Fursenko, R. V.** Characteristics of microscale combustion in a narrow heated channel. *Combust. Explos. Shock Waves*, 2004, **40**(5), 516–523.

18 **Veeraragavan, A., Dellimore, K.,** and **Cadou, C.** Simplified heat transfer analysis for flames in channels. Proceedings of the *39th AIAA thermophysics conference*, American Institute of Aeronautics and Astronautics, Miami, FL, June 25–28 Paper No. AIAA paper 2007-3899.

APPENDIX

Notations

A	cylinder radius (m)
A_n	Fourier series coefficient
B	dust mass concentration (g/m^3)
B_n	Fourier series coefficient
C_n	Fourier series coefficient
c_p	specific heat of gas (kJ/(kg K))
c_s	specific heat of solid (kJ/(kg K))
d_c	tube diameter (m)
d_p	particle diameter (μm)
E_n	Fourier series coefficient
F_n	Fourier series coefficient
J_0	Bessel function of the first kind of order 0
J_1	Bessel function of the first kind of order 1
J_2	Bessel function of the first kind of order 2
M	mass of particle (g)
N	parameter defined in equation (7)
Q	heat of reaction per unit mass of fuel (kJ/kg)
r_s	particle radius (μm)
R	radial coordinate
S	parameter defined in equation (7)
t_n	Fourier series coefficient
T	temperature of the gas phase (K)
T_s	temperature of the solid phase (K)
V	flame speed (cm/s)
W_f	heat source term defined in equation (2)
Z	horizontal coordinate

Greek symbols

α_n	parameter defined in equation (15)
β_n	parameter defined in equation (15)
γ_n	parameter defined in equation (15)
ζ	parameter defined in equation (17)
θ	parameter defined in equation (7) (K)
θ_s	parameter defined in equation (17) (K)
λ	thermal conductivity of gas (W/(m K))
μ_n	eigenvalues
$\varphi = B/B_{st}$	equivalence ratio
ρ	density of the gas phase (kg/m^3)
ρ_s	density of the solid phase (kg/m^3)
τ_c	burning time (s)

Subscripts

S	solid phase
Si	shows solid particle at the beginnings of burning
St	stoichiometric condition
U	characteristics of unburned mixture at $z = -\infty$